Symmetry-based Transport Theory of Monolayer Transition-Metal Dichalcogenides

Yang Song[1,*] and Hanan Dery[2,1]

[1]*Department of Physics and Astronomy, University of Rochester, Rochester, New York, 14627*
[2]*Department of Electrical and Computer Engineering, University of Rochester, Rochester, New York, 14627*

We present a general group-theoretical scheme for the transport in monolayer transition-metal dichalcogenides. The theory elucidates the major momentum and spin relaxation processes for electrons, holes and hot excitons. We expatiate on spin flips induced by flexural phonons and show that the spin relaxation is ultrafast in free-standing membranes while being mitigated in supported membranes. This behavior is universal in 2D membranes that respect mirror symmetry and it leads to a counterintuitive inverse relation between mobility and spin relaxation.

PACS numbers:

Single-layer transition-metal dichalcogenides (SL-TMDs) put together exotic charge, spin and valley electronic phenomena [1, 2]. Recent advances in the exfoliation and fabrication of these materials have sparked a wide interest in their d-band semiconducting behavior and spin-valley coupling [3–6]. Room-temperature mobility of the order of 100 $cm^2/V{\cdot}s$ in single-layer n-type MoS_2 transistor was demonstrated and analyzed [7–9]. In addition, the unique time-reversal relations between spin and valley degrees of freedom were studied from the circular polarization of the exciton photoluminescence (PL) [10–13]. In spite of these recent advances and supporting studies of band-structure and phonons parameters [14–19], there is still no unifying description of the spin and charge transport in these intriguing materials.

In this Letter, we present a group-theoretical analysis of SL-TMDs. The theory elucidates pertinent momentum and spin relaxation mechanisms, and places the physics of charge, spin and exciton transport on a firm footing. We first delineate the transport limitations at elevated temperatures via zeroth-order selection rules and make connection with the energy relaxation of hot excitons. It is shown that spin-conserving scattering between direct and indirect exciton bands leads to reduction in the circular polarization degree of the PL. Then, we analyze the intricate physics of spin relaxation due to scattering with long-wavelength flexural phonons and compare the findings with the case of graphene. Ultrafast spin relaxation is predicted for free-standing and suspended SL-TMDs whereas for supported membranes the spin lifetime is greatly enhanced. Finally, we discuss the relation between spin relaxation and charge mobility.

Figure 1(a) shows the trigonal prismatic lattice structure of monolayer MX_2 where M (X) denotes the transition-metal (chalcogen) atom. Essential parts of the energy bands are sketched in Fig. 1(b). The lack of space-inversion center lowers the symmetry from point-group D_{6h} to D_{3h}, leading to spin-split energy bands and to complex irreducible representations (IRs) of general points in **k**-space [20]. The IRs of high-symmetry points, shown in Fig. 1(b), provide useful insights to transport

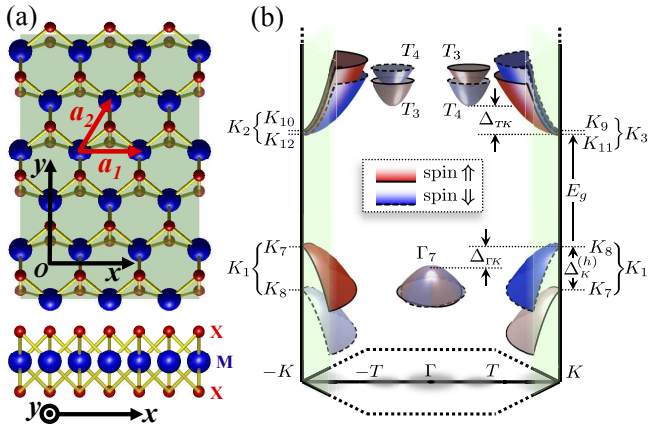

FIG. 1: (Color online) (a) Top and side views of the real space lattice. (b) Typical scheme of primary and satellite valleys in the conduction and valence bands. As implied from the strict one-dimensional irreducible representations of the double group, all bands in the K point are spin-split [20].

and optical properties. We begin with the lowest-order processes characterized by nonvanishing phonon-induced scattering between valley centers, and by a temperature dependence that follows the phonon population (Bose-Einstein distribution in equilibrium) [21]. Table I lists the lowest-order selection rules from which all of the nonvanishing phonon symmetries are found. These modes are visualized in Fig. 2 for the cases of zone-center and zone-edge phonons. With the exception of Γ_4 that corresponds to zeroth-order spin flips in the T valleys, energies of all other phonon modes are non-negligible [20]. Accordingly, charge or spin transport in the K valleys is affected by zeroth-order processes only at elevated temperatures. We summarize their properties below.

The intravalley relaxation of either electrons or holes is induced by homopolar scattering due to an out-of-phase displacement of the two chalcogen atomic layers. As shown in Fig. 2(a) and (b) for the respective cases of momentum and spin relaxation, the effective charge dipole from these long-wavelength displacements is zero

TABLE I: Zeroth-order selection rules in MX_2 compounds. For spin-conserving scattering, double-group IRs are replaced with simpler single-group IRs. Time reversal symmetry connects K and $-K$ points (e.g., K_9=K^*_{10} and K_2=K^*_3).

Valleys	spin-conserving	spin-flip
Intra	$(X \times X^*)^* = \Gamma_1$	$(K_{11} \times K_9^*)^* = \Gamma_5$
	$X = \{K_{1-3}, T_1, \Gamma_1\}$	$(T_3 \times T_4^*)^* = \Gamma_4$
Inter	$(K_3 \times K_2^*)^* = K_3$	
	$(K_1 \times K_1^*)^* = K_1$	
	$(T_1 \times K_3^*)^* = T_1$	$(T_3 \times K_9^*)^* = T_2$
	$(\Gamma_1 \times K_1^*)^* = K_1$	$(\Gamma_{7\uparrow(\downarrow)} \times K^*_{8(7)})^* = K_{5(6)}$

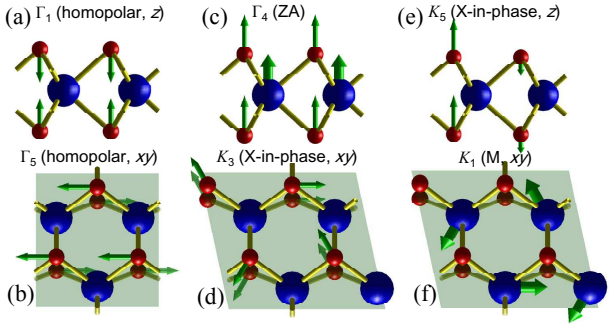

FIG. 2: (Color online) Atomic displacements of the Γ and K phonon modes involved in zeroth-order scattering.

so that the relaxation is governed by a short-range scattering potential. The intravalley momentum relaxation is caused by thickness fluctuations of the layer due to the out-of-plane motion of the chalcogen atoms [Fig. 2(a)]. This physical picture was first identified by Fivaz and Mooser [14], and supported by *ab initio* calculations of Kaasbjerg *et al*'s who also showed a comparable contribution to the charge mobility from Fröhlich interaction [9]. Zeroth-order spin flips in the K valleys are enabled uniquely by homopolar in-plane optical phonons which do not exist in graphene structures [Fig. 2(b)].

The intervalley scattering between primary and satellite valleys ($K\times T$ & $K\times\Gamma$) is relevant due to the flat nature of the d bands in SL-TMDs. This scattering is likely to facilitate the Gunn effect when applying a large in-plane electric field [22]. Namely, accelerated carriers are scattered to the satellite valleys in which the mobility and spin relaxation rates are different [23, 24]. MX_2 compounds with heavy (light) chalcogen atoms have a relatively small Δ_{TK} ($\Delta_{\Gamma K}$) energy spacing [17], and therefore can be used as n-type (p-type) Gunn diodes.

The lowest-order processes in the one-particle picture are completed with the nonvanishing scattering between K and $-K$ valleys. The selection rules show that such scattering largely affects the charge but not the spin transport. The lowest-order spin-flip of either electrons

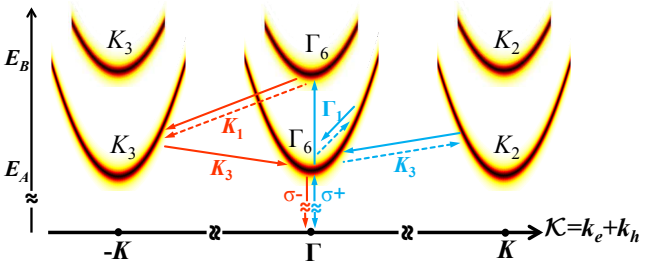

FIG. 3: (Color online) Direct and indirect exciton bands. The optical and exciton-phonon scattering processes are sketched under σ_+ photon excitation. Real (virtual) scattering is denoted by solid (dash) lines and phonon IRs are marked. Right blue (left red) paths lead to $\sigma_+(\sigma_-)$ luminescence.

or holes is forbidden by time reversal symmetry. The conduction-band rule ($K_3\times K_2^*$) is relevant for electron transport in n-type monolayers [9]. The valence-band rule ($K_1\times K_1^*$), however, is likely to affect less the transport of holes due to the relatively large energy splitting ($K_8 \leftrightarrow K_8$ or $K_7 \leftrightarrow K_7$ intervalley transitions in Fig. 1).

As an important application, we show that spin-conserving scattering between K and $-K$ valleys is imperative for understanding recent exciton PL measurements [10–13]. Figure 3 shows the exciton bands of singlet composites ('bright excitons'), where upper and lower branches are due to the valence-band spin splitting [25]. The zone-center bands comprise electron and hole states of the same K valley (direct excitons), where each of the doubly-degenerate zone-center states transform as Γ_6 and include m_l=$\pm$1 excitons depending on light helicity. Zone-edge bands, on the other hand, belong to $K_{2,3}$ and comprise electrons and holes from different valleys (indirect excitons). In the supplemental material we quantify the circular polarization degree of the PL by modeling the absorption and relaxation processes that precede recombination. Here, we summarize this physics and show the relation with selection rules. First, when the exciting photon energy is between E_A and E_B (Fig. 3), both upper and lower bands are excited due to energy broadening by impurities and substrate imperfections [10, 11, 13]. Second, the phonon-assisted indirect absorption, a second-order process shown by dashed arrows in Fig. 3, cannot be neglected since it has many more available final states compared with the direct absorption that is limited to $\boldsymbol{\mathcal{K}} = \mathbf{k}_e + \mathbf{k}_h = 0$ [26]. Third, the intervalley scattering during the relaxation from the upper to lower Γ_6 band flips m_l without a spin-flip of the electron or hole [27]. The missing angular momentum is carried by K_1 and K_3 phonons, as implied from Table I and visualized in Fig. 3 for σ_+ excitation. This rapid relaxation explains the measured reduction in the circular polarization degree [13], and it is enabled in multivalley direct-gap SL-TMDs due to the (so-far ignored) unique coexistence of direct and indirect exciton bands.

In the remainder of the Letter, we study the transport due to interaction with long-wavelength acoustic phonons. As in other materials, the vanishing energies of these phonons render this nonzero-order interaction important. We first mention the fundamental distinction between charge and spin transport in monolayers that respect mirror symmetry (e.g., graphene and SL-TMDs). For interactions with single phonons, spin-conserving scattering is not affected by long-wavelength flexures in the out-of-plane direction [28], whereas spin-flip scattering induced by flexural phonon does not vanish [the ZA mode in Fig. 2(c)]. Mathematically, it is understood from the scattering integral, $\langle \mathbf{s}_f|\nabla\mathcal{V}|\mathbf{s}_i\rangle$, where in-plane $\partial\mathcal{V}/\partial r_\parallel$ (out-of-plane $\partial\mathcal{V}/\partial z$) deformations are even (odd) with respect to mirror symmetry which also brings in ±1 for $\mathbf{s}_i=\pm\mathbf{s}_f$.

To compactly express the scattering rates we employ the invariant method [29]. The transition amplitudes for spin-conserving scattering with in-plane long-wavelength acoustic phonons in the Γ, K or T valleys are

$$\mathcal{T}^{sc}_{\lambda,\mathbf{q}}=\sqrt{\frac{k_BT}{2\varrho A v_\lambda^2 q^2}}\begin{cases}\Xi_{\Gamma_1}\boldsymbol{\xi}_\lambda\cdot\mathbf{q},\\ \Xi^d_{K_{1(3)}}\boldsymbol{\xi}_\lambda\cdot\mathbf{q}+\Xi^o_{K_{1(3)}}(\boldsymbol{\xi}_\lambda\times\mathbf{q})_z,\\ \Xi^{\alpha\beta}_{T_1}\xi_{\lambda,\alpha}q_\beta,\end{cases} \quad (1)$$

where ϱ, A and v_λ are the areal mass density, area, and mode-dependent sound velocity, respectively. $\mathbf{q}=\mathbf{k}_f-\mathbf{k}_i$ is the small wavevector difference between the initial and final states. Summation over tensor components is implied in the T-valley. Typical values of components of the deformation-potential tensor (Ξ) are a few eV [9, 20]. Employing the isotropic model for the phonon polarization vectors, $\boldsymbol{\xi}_{TA}=(q_y,-q_x)/q$ and $\boldsymbol{\xi}_{LA}=\mathbf{q}/q$, one can resolve the contributions of in-plane transverse and longitudinal acoustic modes.

The spin-flip transition amplitudes from scattering with long-wavelength flexural phonons ($\xi_z\approx1$) are

$$\mathcal{T}^{sf}_{ZA,\mathbf{q}}\approx\sqrt{\frac{k_BT}{2\varrho A}}\frac{g(\mathbf{k}_i,\mathbf{k}_f)}{\gamma^2q^{2\eta}}\,, \quad (2)$$

where γ and η are mechanically-dependent parameters that set the flexural-phonon dispersion. Their values will be introduced when estimating the spin lifetimes in different monolayer conditions. $g(\mathbf{k}_i,\mathbf{k}_f)$ can be replaced by $\Xi^{so}_{\Gamma_1}|\mathbf{k}_i+\mathbf{k}_f|q$ in the zone-center, by $\Xi^{so}_K q$ in the zone-edge, or by $\Xi^{so}_{T_1}$ in-between, where Ξ^{so}_X are spin-orbit coupling scattering constants. The linear wavevector dependence in the K valley enables estimation of Ξ^{so}_K from spin-dependent energy changes in the band structure when applying static strain. By symmetry, shear-strain components of the form $\epsilon_\pm=\epsilon_{xz}\pm i\epsilon_{yz}$ are associated with frozen flexural phonons, and by focusing on the spin dependent part of the static strain Hamiltonian at $\mathbf{k}=\mathbf{K}$,

$$H_0+H^{so}(\epsilon_+)=\begin{pmatrix} b|\epsilon_+|^2 & a\epsilon_+\\ a\epsilon_- & \Delta_K-b|\epsilon_+|^2\end{pmatrix}, \quad (3)$$

we find that $a=\Xi^{so}_K$ [20]. a and b are spin-dependent shear deformation potentials, and Δ_K is the spin splitting without strain. The underlying physics is similar for K points in the conduction or valence bands. The value of Ξ^{so}_K, needed for estimation of the spin relaxation, can now be readily extracted from the strain-induced spin splitting $\sqrt{(\Delta_K+2b|\epsilon_+|^2)^2+|2a\epsilon_+|^2}$. Using ABINIT (an open-source DFT code) with Hartwigsen-Goedecker-Hutter pseudopotentials, we find that $\Xi^{so}_K\approx0.2$ eV in the conduction band of monolayer MoS_2 [30], and ~0.1 eV in its valence band [20]. A notable feature in the conduction band of SL-TMDs is that Δ_K can be much smaller than Ξ^{so}_K. Their decoupled nature explains the difference: Δ_K is induced by small contribution from chalcogen atoms [17], and Ξ^{so}_K by *interband* spin-orbit coupling that involves the d_{z^2} orbital of the transition-metal atom.

Having values of the spin-dependent scattering constants, we quantify the K-valley spin relaxation rate due to interaction with flexural phonons [Eq. (2)]. To account for the spin splitting, the top valley is indexed by t and the lower one by ℓ. For elastic scattering from $\ell(t)$ to $t(\ell)$, the spin-flip rate of the $\mathbf{k}$-state is

$$\tau^{-1}_{sf}(\mathbf{k})\approx\frac{2m_{t(\ell)}(\Xi^{so}_K)^2k_BT}{\hbar^3\varrho\gamma^2(k'+k)^{2\eta-2}}\cdot{}_2F_1\Big(\tfrac{1}{2},\eta-1;1;\tfrac{4kk'}{(k+k')^2}\Big), \quad (4)$$

where $k'=\sqrt{m_{t(\ell)}k^2/m_{\ell(t)}+(-)2m_{t(\ell)}\Delta_K/\hbar^2}$ and $m_{t(\ell)}$ is the effective mass. The hypergeometric function can be recast to simpler forms for case-specific η values. The respective expression for T valley spin flips is similar in form to (4), but with $\eta\to\eta+1$ which reflects faster spin relaxation (as implied from its zeroth-order selection rule; see Table I). We continue the analysis and calculate the K-valley spin relaxation rate in two limiting cases.

free-standing monolayers. Without a stiffening mechanism to suppress violent undulations, 2D membranes would crumple [31]. In crystal monolayers, this mechanism is naturally provided by the coupling between bending and stretching degrees of freedom. To lowest order in the coupling, the long-wavelength phonon dispersion is renormalized from $\eta=2$ to $\eta=3/2$ and $\gamma=\sqrt[4]{k_BT/\varrho v_0^2}$ where $v_0\approx v_{TA}\sqrt{1-v^2_{TA}/v^2_{LA}}$ [28, 31]. Assuming similar masses ($m_K=m_t=m_\ell$), the effective spin relaxation rate for Boltzmann distribution becomes

$$\frac{1}{\tau_s}=\sqrt{\frac{8\pi m_K}{\varrho v_o^2}}\left(\frac{\Xi^{so}_K}{\hbar}\right)^2\left[\frac{\mathrm{Erfc}(\sqrt{\beta_K})}{1+e^{-\beta_K}}\left(1+\frac{0.1}{\sqrt{\beta_K}}\right)\right], \quad (5)$$

where $\beta_K=\Delta_K/k_BT$. Due to a relatively large valence-band splitting, the $\beta_K>1$ limit applies for holes at all practical cases where the temperature dependence is largely set by the complementary error function. Furthermore, in compounds with heavier transition-metal atoms (larger splitting), the flexural induced spin relaxation of holes is slower in spite of a larger Ξ^{so}_K. For example, in MoS_2 where $\Delta^{(h)}_K=160$ meV and in WS_2

where $\Delta_K^{(h)} = 450$ meV [17], the respective spin lifetimes at 300 K are, respectively, ~ 0.2 ns and ~ 2 μs [32]. In addition to scattering with flexural phonons, the intrinsic spin relaxation of holes is affected by intravalley scattering with in-plane homopolar phonons [Fig. 2(b)], or by intervalley scattering between K and $-K$. Whereas the latter spin-flip scattering is forbidden in the zeroth-order by time reversal symmetry (Table I), it is not impeded by the relatively large spin splitting. Signatures of the homopolar and intervalley spin-flip mechanisms can be observed from their temperature dependence (Bose-Einstein distribution of the involved phonons).

The spin relaxation of electrons is much faster due to the small spin splitting in the conduction band. In MoS_2 where $\Delta_K^{(e)} = 4$ meV [19], the room-temperature spin lifetime is $\tau_s \sim 0.05$ ps [32], and it increases noticeably only below 50 K. Interestingly, the spin relaxation of electrons is enhanced in compounds with lighter chalcogen atoms (their weaker spin-orbit coupling leads to smaller $\Delta_K^{(e)}$). Furthermore, the spin relaxation diverges in the pathological limit of $\Delta_K^{(e)} \to 0$ [33]. Finally, repeating the analysis for suspended monolayers by employing $\eta = 1$ and $\gamma = v_0\sqrt{\bar{\epsilon}}$, we find that $\tau_s < 1$ ps at room-temperature even for suspension-induced strain levels of $\bar{\epsilon} \sim 1\%$.

supported monolayers. Another means to stiffen the membrane is naturally provided by van der Waals (vdW) interactions when the monolayer is placed on a substrate [34]. The support brings in a minimum cutoff energy for out-of-plane displacements. The cutoff energy, $\Omega_c = \hbar\sqrt{\kappa_s/M_u}$, is calculated from the average vdW interatomic force constant between the monolayer and the substrate (κ_s), and the average atomic mass of the monolayer (M_u). In the long-wavelength limit, we can therefore approximate the dispersion of flexural phonons by $\eta = 0$ and $\gamma = \Omega_c/\hbar$. The effective spin relaxation rate becomes

$$\frac{1}{\tau_s} = \frac{(2m_K\Xi_K^{so})^2}{\hbar^3\varrho}\cdot\frac{4+2\beta_K}{(1+e^{\beta_K})\beta_c^2}\,, \qquad (6)$$

$\beta_c = \Omega_c/k_BT < 1$ is assumed. The temperature dependence is quadratic for $\beta_c < \beta_K < 1$ and exponential for $\beta_c < 1 < \beta_K$. The substrate coupling brings in slower relaxation which at room temperature reaches $\tau_s \sim 7$ ps (~ 1 ns) for electrons (holes) in supported MoS_2 with $\Omega_c = 1$ meV [35]. The spin-lifetime enhancement from $\eta = 3/2$ to $\eta = 0$ is sharper for electrons due to the smallness of $\Delta_K^{(e)}$ compared with $\Delta_K^{(h)}$. As a result, phonons of longer wavelength are involved in energy-conserving spin flips in the conduction band.

We compare the spin relaxation induced by flexural phonons in graphene and MX_2. The space inversion symmetry in graphene mandates spin-degenerate energy bands, resulting in anisotropic relaxation that depends on the spin orientation. Defining the latter by out-of-plane polar angle ($\theta_{\mathbf{s}}$) and in-plane azimuthal angle ($\phi_{\mathbf{s}}$), the spin-flip transition amplitude due to elastic scattering with flexural phonons follows (2) where

$$g(\mathbf{k}_i,\mathbf{k}_f) = ik\Xi_{\boldsymbol{\kappa}}^{so}\sin^2\phi_-\left[\sin^2\frac{\theta_{\mathbf{s}}}{2}e^{2i\phi_{\mathbf{s}}-i\phi_+} + \cos^2\frac{\theta_{\mathbf{s}}}{2}e^{i\phi_+}\right]. \qquad (7)$$

The other angles, $\phi_\pm = \frac{1}{2}(\tan^{-1}\frac{k_{x,f}}{k_{y,f}} \pm \tan^{-1}\frac{k_{x,i}}{k_{y,i}})$, are due to the Dirac-cone energy dispersion. Formal analytical derivation of this result will be presented in a future long publication. Here we mention that the prefactor $k\sin^2\phi_- = q^2/4k$, previously found by numerical techniques [36], originates from space-inversion symmetry and spin-dependent energy dispersion in the cone region. Away from the Dirac point (k=0), the spin relaxation timescales are longer in graphene than in SL-TMDs on accounts of the higher power-law in phonon wavevector (q^2 vs q) and the relative smallness of $\Xi_{\boldsymbol{\kappa}}^{so}$ in carbon-based systems (~ 10 meV [37]).

All these findings lead to a counterintuitive relation between charge mobility and spin relaxation in 2D membranes. Whereas increased stiffness has been shown to be associated with slower spin relaxation, its coupling with charge mobility seems to have the opposite trend. For example, high mobility in supported membranes is a token of diminished effect from adsorbents and substrate imperfections. A smaller coupling of the membrane to such parasitics would enable freer and softer out-of-plane undulations. Therefore, an inverse trend between spin and momentum relaxation, a hallmark of Dyakonov-Perel spin dephasing processes, can be realized in a Elliott-Yafet spin flip system (scattering with flexural phonons). This physics is universal in relatively clean 2D membranes that respect mirror symmetry. In such membranes, charge transport is decoupled from harmonic out-of-plane undulations while spin relaxation is not severely affected by the presence of impurities.

In conclusion, we have presented a transparent theory of intrinsic transport properties in single-layer transition-metal dichalcogenides. Lowest-order scattering processes were identified in both charge and spin transport regimes, and were found relevant to the transport of free-carriers at elevated temperatures and for the energy relaxation of hot excitons. As a group-theoretical study, findings of previous important theories were mentioned as special cases. In addition, the spin relaxation induced by scattering with long-wavelength flexural phonons was quantified. For electrons, the ultrafast rate is attributed to the typical softness of 2D membranes and to the small spin splitting in the conduction band. The relatively large splitting in the valence band, on the other hand, renders p-type monolayers better candidates for preserving spin information.

We are indebted to Professor Walter Lambrecht and Mr. Tawinan Cheiwchanchamnangij for insightful discussions and for sharing frozen-phonon DFT results prior to their publication. This work is supported by NRI-NSF, NSF, and DTRA Contract numbers DMR-1124601, ECCS-1231570, and HDTRA1-13-1-0013, respectively.

* Electronic address: yang.song@rochester.edu

[1] D. Xiao, G.-B. Liu, W. Feng, X. Xu, and W. Yao, Phys. Rev. Lett. **108**, 196802 (2012).

[2] S. Cahangirov, C. Ataca, M. Topsakal, H. Sahin, and S. Ciraci, Phys. Rev. Lett. **108**, 126103 (2012).

[3] K. F. Mak, C. Lee, J. Hone, J. Shan, and T. F. Heinz, Phys. Rev. Lett. **105**, 136805 (2010).

[4] A. Splendiani, L. Sun, Y. Zhang, T. Li, J. Kim, C.-Y. Chim, G. Galli, and F. Wang, Nano Lett. **10**, 1271 (2010).

[5] T. Korn, S. Heydrich, M. Hirmer, J. Schmutzler, and C. Schüller, Appl. Phys. Lett. **99**, 102109 (2011).

[6] T. Cao, G. Wang, W. Han, H. Ye, C. Zhu, J. Shi, Q. Niu, P. Tan, E. Wang *et al.*, Nat. Comm. **3**, 887 (2012).

[7] B. Radisavljevic, A. Radenovic, J. Brivio, V. Giacometti, and A. Kis, Nat. Nano. **6**, 147 (2011).

[8] S. Kim, A. Konar, W.-S. Hwang, J. H. Lee, J. Lee, J. Yang, C. Jung, H. Kim, J.-B. Yoo *et al.*, Nat. Comm. **3**, 1011 (2012).

[9] K. Kaasbjerg, K. S. Thygesen, and K. W. Jacobsen, Phys. Rev. B. **85**, 115317 (2012).

[10] H. Zeng, J. Dai, W. Yao, D. Xiao, and X. Cui, Nat. Nano. **7**, 490 (2012).

[11] K. F. Mak, K. L. He, J. Shan and T. F. Heinz, Nat. Nano. **7**, 494 (2012).

[12] G. Sallen, L. Bouet, X. Marie, G. Wang, C. R. Zhu, W. P. Han, Y. Lu, P. H. Tan, T. Amand *et al.*, Phys. Rev. B **86**, 081301(R) (2012).

[13] G. Kioseoglou, A. T. Hanbicki, M. Currie, A. L. Friedman, D. Gunlycke, and B. T. Jonker, Appl. Phys. Lett. **101**, 221907 (2012).

[14] R. Fivaz and E. Mooser, Phys. Rev. **163**, 743 (1967).

[15] A. Wilson and A. D. Yoffe, Adv. Phys. **18**, 193 (1969).

[16] L. F. Mattheiss, Phys. Rev. B. **8**, 3719 (1973).

[17] Z. Y. Zhu, Y. C. Cheng, and U. Schwingenschlögl, Phys. Rev. B **84**, 153402 (2011).

[18] A. Molina-Sánchez and L. Wirtz, Phys. Rev. B. **84**, 155413 (2011).

[19] T. Cheiwchanchamnangij and W. R. L. Lambrecht, Phys. Rev. B **85**, 205302 (2012).

[20] See supplemental material for character tables, association of states with irreducible representations, integrals of scattering constants, and optical properties of excitons.

[21] Y. Song and H. Dery, Phys. Rev. B **86**, 085201 (2012).

[22] J. Gunn, IBM J. Res. Dev. **8**, 141 (1964).

[23] H. Kroemer, Proc. IEEE **52**, 1736 (1964).

[24] J. Li, L. Qing, H. Dery, and I. Appelbaum, Phys. Rev. Lett. **108**, 157201 (2012).

[25] The reduced screening in 2D renders a relatively large exciton binding energy such that $E_{A,B}$ in Fig. 3 lies well below the one-particle energy gaps [11, 19].

[26] R. J. Elliott, Phys. Rev. **108**, 1384 (1957).

[27] In addition, spin flops due to electron-hole exchange (Bir-Aronov-Pikus mechanism) are typically too slow to account for the measured reduction in the circular polarization degree (see supplemental material in [11]).

[28] E. Mariani and F. von Oppen, Phys. Rev. Lett. **100**, 076801 (2008).

[29] G. L. Bir and G. E. Pikus, *Symmetry and Strain-induced Effects in Semiconductors* (Halsted Press, Jerusalem, 1974), Chapters 3-4.

[30] Independently, Tawinan Cheiwchanchamnangij and Walter Lambrecht got similar results by using a full-potential linearized muffin-tin orbital method (unpublished).

[31] D. R. Nelson and L. Peliti, J. Phys. (Paris) **48**, 1085 (1987).

[32] In MoS_2: $\varrho = 3.1\times10^{-7}$ gr/cm^2 and $v_{TA(LA)} = 4.2(6.7)\times 10^5$ cm/s [9]. For electrons (holes): $m_K = 0.34m_0$ ($0.45m_0$) and $\Delta_K = 4$ meV (160 meV) [19]. Inferred from the atomic spin splitting of W and Mo, we assume that Ξ_K^{so} of WS_2 is $\sim$3.5 times larger than that of MoS_2.

[33] We note that electrons hardly change trajectory during spin-flip scattering with long-wavelength flexural phonons ($q \to 0$). These spin-flips are therefore ineffective in reducing mobility.

[34] J.-H. Seol, I. Jo, A. L. Moore, L. Lindsay, Z. H. Aitken, M. T. Pettes, X. Li, Z. Yao, R. Huang *et al.*, Science **328**, 213 (2010).

[35] We assumed a force constant of ~ 0.4 N/m, similar to the one found in graphene on SiO_2 [34].

[36] S. Fratini, D. Gosálbez-Martnez, P. Merodio Cámara, J. Fernández-Rossier, arXiv:1202.6216 (2012).

[37] D. Huertas-Hernando, F. Guinea, and A. Brataas, Phys. Rev. B **74**, 155426 (2006).